Vibrational Relaxation of $SO(X^3\Sigma^-, v = 1-5)$ and Nascent Vibrational Distributions of SO Generated in the Photolysis of SO_2 at 193.3 nm

Katsuyoshi Yamasaki,* Fumikazu Taketani, Kazuyuki Sugiura, and Ikuo Tokue
Department of Chemistry, Niigata University, Ikarashi, Niigata 950-2181, Japan

Kentaro Tsuchiya
National Institute of Advanced Industrial Science and Technology, 16-3 Onogawa Tsukuba Ibaraki 305-8569, Japan

Received: November 3, 2003; In Final Form: January 18, 2004

Rate coefficients for deactivation of $SO(X^3\Sigma^-, v = 1-5)$ by collisions with SO_2 and nascent vibrational populations in $v = 0-2$ in the photolysis of SO_2 at 193.3 nm have been determined. A single vibrational level of $SO(X^3\Sigma^-)$ was detected with laser-induced fluorescence (LIF) excited via the $B^3\Sigma^- - X^3\Sigma^-$ system. Time-dependent profiles of LIF signals were recorded as a function of the pressures of SO_2. Observed profiles were analyzed by the integrated-profiles method and reproduced well by convolution calculations. Overall rate coefficients for vibrational relaxation of $SO(v)$ by SO_2 have been determined to be $(4.7 \pm 0.5) \times 10^{-12}$ ($v = 1$), $(6.7 \pm 0.4) \times 10^{-12}$ ($v = 2$), $(7.2 \pm 0.7) \times 10^{-12}$ ($v = 3$), $(6.1 \pm 1.0) \times 10^{-12}$ ($v = 4$), and $(8.6 \pm 0.7) \times 10^{-12}$ ($v = 5$) in units of cm^3 $molecule^{-1}$ s^{-1} (the quoted errors are 2σ). We have also found that 63% of the vibrational deactivations of $v = 2$ by SO_2 are governed by double-quantum relaxation: $(4.2 \pm 0.9) \times 10^{-12}$ cm^3 $molecule^{-1}$ s^{-1} for $v = 2 \rightarrow v = 0$ and $(2.5 \pm 0.9) \times 10^{-12}$ cm^3 $molecule^{-1}$ s^{-1} for $v = 2 \rightarrow v = 1$. Ab initio calculations enable us to find two stable complexes: OS−OSO and SO−SO_2, indicating that attractive interactions play a significant role in the relaxation. The nascent vibrational distributions of SO have been measured to be $0.52 \pm 0.1/0.75 \pm 0.1/1.0$ for $v = 0/1/2$. The differences in vibrational distributions reported by bulk and beam experiments are attributed to the difference in the temperature of parent SO_2.

Introduction

The SO radical has attracted the attention of many researchers, because SO plays an important role in combustion systems of sulfur-containing compounds.[1] SO is also a key species of chemical processes following photodissociation of SO_2 in the atmospheres of earth,[2] planets,[3] and interstellar clouds.[4] There have been several reports on the nascent vibrational energy distributions of $SO(X^3\Sigma^-)$ generated in the photolysis of SO_2 at 193 nm.[5−12] All the studies agree that vibrational distributions peak at $v = 2$ and that most of the SO is populated in the levels $v \leq 2$. There, however, have been unsolved discrepancies in vibrational distributions and generation of high vibrational levels $v = 4$ and 5.

Kanamori et al.[7] measured vibrational distributions by tunable infrared diode-laser spectroscopy, reporting that there are a few percent populations in $v = 5$ in contrast to no population in $v = 4$. They have also found that rotational distributions differ from thermal distributions and that higher rotational levels are populated in lower vibrational states. Kolbe and Leskovar[8] detected SO by millimeter-wave rotational spectroscopy and reported that the relative population of $v = 5$ is about 2%. They, however, made no measurement of $v = 4$ and simply assumed no population in $v = 4$. In contrast to these studies, Chen et al.[11] have reported no populations in $v \geq 3$. They employed the laser-induced fluorescence (LIF) technique to detect SO and assigned observed peaks to the rovibrational transitions via the $A^3\Pi - X^3\Sigma^-$ system. Photofragment time-of-flight (TOF) mass translational spectroscopy employed by several groups[9,10,12] has given clear evidence of inverted distributions over $v = 0-2$. However, photofragments with high vibrational energies ($v = 4$ and 5) have too small kinetic energy to detect by the TOF technique. Felder et al.[10] have concluded that about 90% of SO fragments are populated in $v = 1$ and 2; on the other hand, Kawasaki and Sato[9] have reported relatively broad distributions over $v = 0-3$ which are similar to those measured in bulk experiments by Kolbe and Leskovar.[8]

There have been few studies on vibrational relaxation of $SO(X^3\Sigma^-)$. Kanamori et al.[7] observed the time evolution of the population in each vibrational level. They, however, did not determine the rate coefficients of vibrational relaxation, because rotational relaxation was not distinguished from vibrational relaxation under their experimental conditions (a few tens of mTorr). Kolbe and Leskovar[8] also recorded time-dependent profiles of populations in vibrational levels. Diffusion loss was too fast in their experiments (< 200 mTorr) to establish quantitative results on vibrational relaxation, although their data indicated that the vibrational relaxation of $v = 2$ in SO_2(5%)/Ar mixture is faster than that of $v = 1$.

In the measurement of rate coefficients for vibrational relaxation, rotational motion must be thermalized sufficiently faster than that of vibration. Inert gases, for example, rare gases and molecular nitrogen, at a few tens of Torr, must be introduced to a system to accelerate rotational relaxation exclusively. In the present study, we have detected $SO(X^3\Sigma^-, v = 0-5)$ by LIF excited via the $B^3\Sigma^- - X^3\Sigma^-$ system and recorded time-dependent profiles as a function of the pressures of SO_2 in a buffer gas at 50 Torr of N_2. We have analyzed the observed data by the integrated-profiles method coupled with convolution calculation based on the linear response theory. This method

* Corresponding author. Fax: +81-25-262-7530. E-mail: yam@scux.sc.niigata-u.ac.jp.

10.1021/jp037333d CCC: $27.50
Published on Web 03/09/2004

TABLE 1: Excited and Observed Vibrational Bands of SO in the $B^3\Sigma^- - X^3\Sigma^-$ System

excited band	excited rotational line[a]	λ_{ex} /nm[b]	observed band	λ_{obs} /nm
0−0	$P_{11}(13) + P_{33}(13)$	241.97	0−12	350.8
1−1	$P_{11}(15) + P_{33}(15)$	245.14	1−14	368.5
2−2	$R(14)$[c]	248.06	2−17	401.2
0−2	$P_{11}(15) + P_{33}(15)$	256.06	0−12	350.8
1−3	$R_{11}(15) + R_{33}(15) + P_{22}(10)$	259.14	1−14	368.5
2−4	$R(17)$[c]	262.58	2−17	401.2
2−5	$R(14)$[c]	270.16	2−17	401.2

[a] The labels of rotational lines are defined to be $\Delta N_{ij}(N'')$, where N is the quantum number of total angular momentum apart from spin and the subscripts i and j represent spin sublevels of upper and lower states. [b] Wavelengths in the air. [c] Spin sublevels are not assigned.

enables us to determine not only the rate coefficients for vibrational relaxation of $SO(X^3\Sigma^-, v = 0-5)$ by collisions with SO_2 but also nascent vibrational distributions immediately following the photolysis. We present evidence that 63% of the vibrational deactivations of $v = 2$ by SO_2 are double-quantum relaxation ($v = 2 \rightarrow v = 0$) and discuss the mechanism of the vibrational relaxation of $SO(X^3\Sigma^-)$ and photodissociation of SO_2.

Experimental Section

The experimental apparatus has been described previously,[13] and specific features for the present study are given here. SO_2 (2−23 mTorr) in a buffer gas (N_2 at 50 ± 0.5 Torr) was introduced to a reaction cell and photolyzed at 193 nm with an ArF excimer laser (Lambda Physik LEXtra50, 19 Hz) at 298 ± 2 K. Vibrational levels of $SO(X^3\Sigma^-, v = 0-5)$ were detected by LIF with a Nd^{3+}:YAG laser (Spectron SL803, 355 nm) pumped frequency-doubled dye laser (Lambda Physik LPD3002 with a BBO I crystal). The vibrational transitions 0−0, $v'-1$, $v'-2$, $v'-3$, 2−4, and 2−5 bands, where $v' = 0-2$, in the $B^3\Sigma^- - X^3\Sigma^-$ system were excited with laser dyes: coumarin 480, LD 489, and coumarin 500. Fluorescence from $SO(B^3\Sigma^-)$ was collected with a quartz lens ($f = 80$ mm) through a UV band-pass filter (Toshiba UV-D35, $T_{max} = 76\%$ at 350 nm, full width at half-maximum (fwhm) = 90 nm) and focused on the photocathode of a high-gain photomultiplier tube (PMT) (Hamamatsu R1104). When spectral congestion needed to be avoided, fluorescence was dispersed with a monochromator (JEOL JSG-125S, $f = 125$ cm, fwhm = 3 nm) and detected with another photomultiplier tube (Hamamatsu R928). The wavelengths of the monochromator were tuned to those of the 0−12 (350.8 nm), 1−14 (368.5 nm), and 2−17 (401.2 nm) bands on excitation to $v' = 0$, 1, and 2, respectively. Fortunately, the three vibrational bands have no overlap with other vibrational bands, which makes it possible to detect a single vibrational level of $SO(X^3\Sigma^-)$. Signals from the PMTs were averaged with a gated integrator (Stanford SR-250, the sampling gate width was 100 ns) and stored on a disk of a PC after A/D conversion (Stanford SR-245).

To record the time profiles of dispersed LIF intensities of a vibrational level, the wavelength of the probe laser was tuned to rotational lines, and then time delays between the photolysis and probe laser were continuously scanned with a homemade delay generator. The wavelengths of excitation and observation are listed in Table 1. The number of data points in a time profile was 2000 with a step size of 1 μs. The buffer gas (N_2) at 50 Torr may be sufficient for instantaneous rotational relaxation, based on the reported rate coefficients for rotational relaxation of SO by various collision partners: 7.8×10^{-10} ($v = 2$) by He,[14] 3.5×10^{-10} ($v = 0$) by Ar,[8] and 2.6×10^{-9} ($v = 0$) by SO_2,[8] in units of cm^3 $molecule^{-1}$ s^{-1}. Rotational states are in thermal equilibrium within at most 2 ns after the photolysis in the present experiments. After rotational motion is thermalized by collisions with a buffer gas, LIF intensity excited via a single rotational line represents the time evolution of the population in a vibrational level of interest.

The $A^3\Pi - X^3\Sigma^-$ transitions of SO may appear over the nearly identical wavelength range with the $B^3\Sigma^- - X^3\Sigma^-$ system,[15−30] and fluorescence via the $A^3\Pi - X^3\Sigma^-$ system was observed in the present experiments. The intensity of the $A^3\Pi - X^3\Sigma^-$ transition, however, was less than 3% in the total fluorescence, which is consistent with relative absorption cross section $\sigma(A^3\Pi \leftarrow X^3\Sigma^-)/\sigma(B^3\Sigma^- \leftarrow X^3\Sigma^-) = 0.027$.[14] Also, photoemission from SO_2 is negligible, because the photoabsorption cross sections of SO_2 at the excitation wavelengths ($\lambda \approx 250$ nm), 1×10^{-19} cm^2,[14,31,32] are smaller than that of $SO(B^3\Sigma^- \leftarrow X^3\Sigma^-)$ by a factor of 2.5×10^4 which more than offsets the concentration ratio $[SO_2]/[SO] \approx 200$ in the present study.

The flow rates of all the sample gases were controlled with calibrated mass flow controllers (Tylan FC-260KZ and STEC SEC-400 mark3) and mass flow sensors (KOFLOC 3810). Linear flow velocity was 10 cm s^{-1} irrespective of buffer gas pressures. Total pressure (N_2 buffer) was monitored with a capacitance manometer (Baratron 122A). The total pressure measurement together with the mole fractions as measured by the flow controllers gave the partial pressures of the reagents. The cylinders of SO_2(3%)/N_2 and N_2 (99.9999%) were delivered by Nihon-Sanso and used without further purification.

Results and Discussion

Laser-Induced Fluorescence Excitation Spectra of SO via the $B^3\Sigma^- - X^3\Sigma^-$ System. Figure 1a shows an LIF excitation spectrum observed with a UV band-pass filter. Because the vibrational constant of the $X^3\Sigma^-$ state of SO, $\omega_e'' = 1150.695$ cm^{-1}, is two times larger than that of $B^3\Sigma^-$, $\omega_e' = 622.5$ cm^{-1},[33] $v'-v''$ bands appear close to $(v' + 2)-(v'' + 1)$ bands. The heads of the $(v' + 2)-(v'' + 1)$ bands are located at shorter wavelength than those of the $v'-v''$ bands, and thus the rotational lines of the $v'-v''$ bands always overlap with those of the $(v' + 2)-(v'' + 1)$ bands. Though seemingly a single band, the spectrum shown in Figure 1a consists of two (0−1 and 2−2) vibrational bands. The rotational transitions of the 4−3 band overlap with those of the 2−2 band; however, vibrational levels $v' \geq 4$ are nonfluorescent because of efficient predissociation by way of the $C^3\Pi$ state.[33,34] To separate the spectrum into the components, dispersed fluorescence via the 0−12 (350.8 nm) and 2−17 (401.2 nm) bands was monitored. Figure 1, parts b and c, shows wavelength-resolved excitation spectra of the 2−2 and 0−1 bands, indicating that such action spectra are useful to detect a single vibrational level.

The $X^3\Sigma^-$ and $B^3\Sigma^-$ states of SO are classified as Hund's case (b) in a good approximation, because $|\lambda|/(2B)$ are 3.6 ($X^3\Sigma^-$) and 3.5 ($B^3\Sigma^-$),[33] where λ is a spin−spin coupling constant and B is a rotational constant.[35] Selection rules for rotational transitions in Hund's case (b) are $\Delta N = \pm 1$ and $\Delta J = 0, \pm 1$, resulting in twelve branches in a $^3\Sigma - ^3\Sigma$ transition: six main branches ($\Delta J = \Delta N$) and six satellite branches ($\Delta J \neq \Delta N$).[36] The intensity of satellite branches falls off rapidly with quantum number N, and consequently, most of the observed rotational lines are assigned to the main branches as shown in the insets of Figure 1, parts b and c.

Vibrational Relaxation of $SO(X^3\Sigma^-, v = 1-5)$ by SO_2. Figure 2 shows the time profiles of the LIF intensities of the

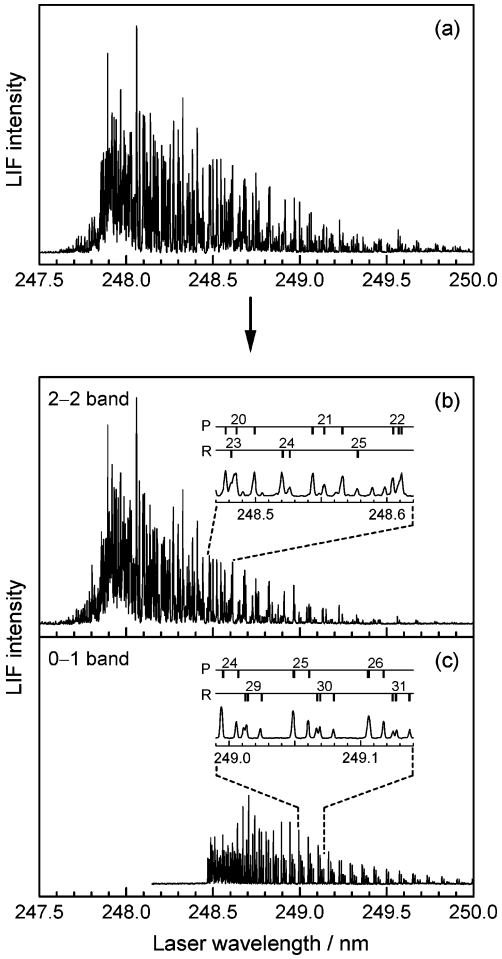

Figure 1. Laser-induced fluorescence excitation spectra of the $B^3\Sigma^- - X^3\Sigma^-$ system of SO. Fluorescence was monitored through a UV band-pass filter, (a); fluorescence was dispersed with a monochromator at 401.2 nm (2−17 band), (b); fluorescence was dispersed with a monochromator at 350.8 nm (0−12 band), (c). $P_{SO_2} = 1.4$ mTorr and $P_{total}(N_2) = 5$ Torr. The delay times between the photolysis and probe laser were 20 μs. The insets in b and c show rotational assignments of the 2−2 and 0−1 bands in the $B^3\Sigma^- - X^3\Sigma^-$ system.

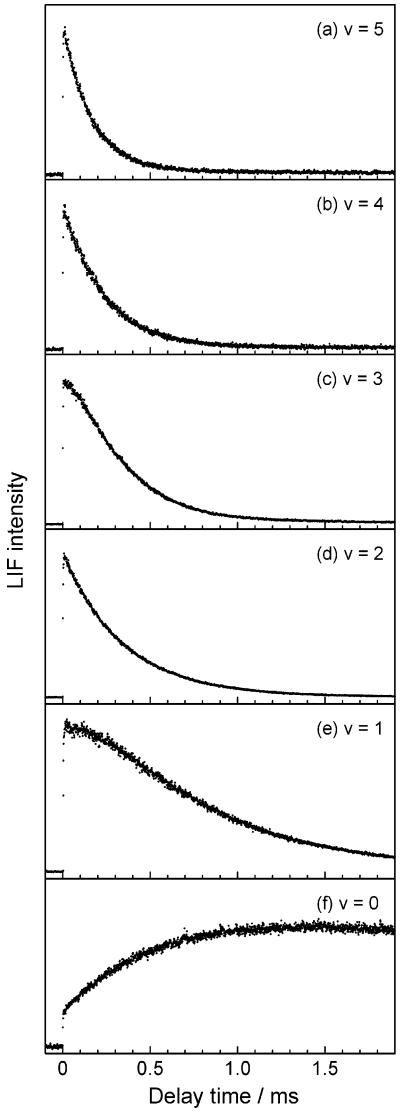

Figure 2. Time-dependent profiles of the LIF intensities of $SO(X^3\Sigma^-, v = 0-5)$. $P_{SO_2} = 7.0$ mTorr and $P_{total}(N_2) = 50$ Torr. The wavelengths of excitation and observation are listed in Table 1. The time axis corresponds to the delay between the photolysis and probe laser pulse. The step size of a time scan is 1 μs, and a single data point represents averaged signals from 10 laser pulses.

vibrational levels of $SO(X^3\Sigma^-, v = 0-5)$ at 50 ± 0.5 Torr (N_2) of total pressure. The available energy that can be deposited into SO fragments is calculated to be 6100 cm^{-1} from the energies of dissociation $D_0(SO-O) = 5.65 \pm 0.1$ eV[37] (45 600 ± 800 cm^{-1}) and the photolyzing light at 193.3 nm (51 733 cm^{-1}). The average electronic energy of the oxygen atoms $O(^3P_J, J = 0, 1,$ and 2), 80 cm^{-1},[38] is negligibly small compared to the confidence limits of the available energy. Parent SO_2 in equilibrium at 298 K has an average internal energy 475 cm^{-1}: the rotational and vibrational energies are 311 cm^{-1} and 164 cm^{-1}, respectively. The line width (fwhm) of the photolysis laser is about 100 cm^{-1}, and thus the highest vibrational level of the SO fragments is $v = 5$ whose term value is 6137 cm^{-1}.[33] Actually, the time profiles of $v = 5$ show single-exponential decay, indicating that the populations in the levels $v > 5$ are negligibly small.

There are some features in the time-dependent profiles. Significant growth seen in the profiles of $v = 0$ shows vibrational relaxation from higher levels. The slightly positive curvatures of $v = 1$ and 3 also show relaxation to these levels. The present study gives the first direct evidence for the production of $v = 4$. No growth in the profiles of $v = 1$ is surprising, because it is well-known that the population in $v = 2$ generated in the photolysis at 193 nm is larger than that in $v = 1$.[7−12] Kinetic analysis must be made to clarify the deactivation mechanism of vibrationally excited SO by collisions with SO_2.

The fates of vibrationally excited $SO(X^3\Sigma^-, v)$ generated in the photolysis are as follows

$$SO(X,v) + M \xrightarrow{k^M_{vv''}} SO(X,v'') + M \quad (1)$$

$$SO(X,v) + SO\ (+M) \xrightarrow{k^{SO}_{rv}} SO_2 + S \text{ or } (SO)_2 + M \quad (2)$$

$$SO(X,v) + O\ (+M) \xrightarrow{k^{O}_{rv}} SO_2\ (+M) \quad (3)$$

$$SO(X,v) + SO_2 \xrightarrow{k^{SO_2}_{rv}} \text{products} \quad (4)$$

$$SO(X,v) \xrightarrow{k_{dv}} \text{diffusion} \quad (5)$$

where $k^M_{vv''}$ is a rate coefficient for vibrational relaxation from v to v'' by collision partners M (M = SO_2 or N_2), k^{SO}_{rv}, k^{O}_{rv}, and $k^{SO_2}_{rv}$ are rate coefficients of reactions with SO, O, and SO_2,

respectively, and k_{dv} is the rate of diffusion loss from the volume irradiated with a probe laser. Rate coefficients of reaction 2 have been reported to be 3.5×10^{-15} cm^3 molecule^{-1} s^{-1} [39] for the products $SO_2 + S$ and 4.4×10^{-31} cm^6 molecule^{-2} s^{-1} [40] for formation of the SO dimer by $M = N_2$. The concentrations of SO and O generated in the present study are estimated to be less than 5×10^{12} cm^{-3} from the experimental conditions: photolysis laser fluence (≤ 1 mJ cm^{-2}) and photoabsorption cross section of SO_2 at 193 nm (7.9×10^{-18} cm^{-2} [14]). The calculated time constants of reaction 2, 57 s ($SO_2 + O$) and 3.5 s [$(SO)_2$], are much longer than the observed decays. Troe's group[41,42] has reported reaction 3 to be in the low-pressure region at 50 Torr of N_2, and the third-order rate coefficients are given to be 7.7×10^{-31} cm^6 molecule^{-2} s^{-1}. The time constant of reaction 3 in the present study is estimated to be 163 ms. Reactions 2 and 3, therefore, are negligible in the present study. Unfortunately, there has been no report on the rate coefficients of reaction 4. We have found that the ratios between the intensity of $v = 0$ immediately following the photolysis and the recovery of the signal, for example, Figure 2f, are independent of the partial pressures of SO_2 within the error limits of $\pm 7\%$. Accordingly, SO appears nonreactive to SO_2 under the present experimental conditions. However, the total population of $v = 3-5$ is very small (less than 10%[7-10,12]), and it cannot be deduced from the recovery of $v = 0$ that SO($v = 3-5$) are nonreactive to SO_2. SO might be regenerated by a reaction of $O + SO_2 \rightarrow SO + O_2$. There, however, has been no kinetic study of this reaction at around room temperature. The rate coefficient at 298 K is tentatively estimated to be 4.3×10^{-26} cm^3 molecule^{-1} s^{-1} by extrapolation using Arrhenius parameters, $A = 8.3 \times 10^{-12}$ cm^3 molecule^{-1} s^{-1} and $E_a = 81.5$ kJ mol^{-1}, effective over the temperature range of 440−3000 K.[43] Regeneration of SO, whose time constant is $\sim 3 \times 10^{10}$ s, is negligible in the present study.

The time profiles of the levels $v \leq 2$ are hardly affected by relaxation from $v \geq 3$, if at all. Actually, the profiles of $v = 2$ show clear single-exponential decay at all pressures of SO_2. First, the time profiles of $v \leq 2$ were analyzed on the assumption of single-quantum relaxation. The rate equation of a given vibrational level is

$$\frac{d[v]}{dt} = (k^{SO_2}_{v+1,v}[SO_2] + k^{N_2}_{v+1,v}[N_2])[v+1] - (k^{SO_2}_{v,v-1}[SO_2] + k^{N_2}_{v,v-1}[N_2] + k_d)[v] \quad (6)$$

where the first term on the right side represents production of a level v from $v + 1$ and the second term corresponds to removal of the level v by relaxation and diffusion. It is assumed that the rates of diffusion loss of different vibrational levels are identical at the same buffer gas pressure. Up-conversion, from v to $v + 1$, can be negligible, because the ratio $k(v+1 \leftarrow v)/k(v+1 \rightarrow v)$ is estimated to be 0.004 from $\omega_e[SO(X^3\Sigma^-)] = 1150.695$ cm^{-1}.[33] The observed LIF intensity of the level v, I_v, is proportionally related to the concentration $[v]$

$$I_v = \alpha_v[v] \quad (7)$$

where α_v is a detectivity of the level v. Substituting eq 7 for the concentrations in eq 6, we obtain the following equation in terms of the observed intensity.

$$\frac{dI_v}{dt} = k_{v+1,v}\frac{\alpha_v}{\alpha_{v+1}}I_{v+1} - (k_{v,v-1} + k_d)I_v \quad (8)$$

where $k_{vv''}$ is an apparent first-order rate of vibrational relaxation from v to v'' at given pressures of SO_2 and buffer gas: $k_{vv''} \equiv k^{SO_2}_{vv''}[SO_2] + k^{N_2}_{vv''}[N_2]$. Integration of eq 8 from $t = 0$ to an arbitrary time t gives[13,44-48]

$$(I_v - I^0_v)/\int_0^t I_{v+1}\,dt' = k_{v+1,v}\frac{\alpha_v}{\alpha_{v+1}} - (k_{v,v-1} + k_d)(I_v/\int_0^t I_{v+1}\,dt') \quad (9)$$

where I^0_v is the LIF intensity immediately after the photolysis. If the plots based on eq 9 for adjacent vibrational levels show linear correlation, the slopes and intercepts of regression lines give the first-order vibrational relaxation rates and relative detectivities. However, none of the plots for $v = 0$ according to eq 9 are linear at any pressure of SO_2, indicating that not only single-quantum vibrational relaxation ($v = 1 \rightarrow v = 0$) but also double-quantum cascade ($v = 2 \rightarrow v = 0$) by collisions with SO_2 must be taken into account. Therefore, the following equations were used to analyze the profiles of $v = 0-2$

$$I_2 - I^0_2 = -(k_{20} + k_{21} + k_d)\int_0^t I_2\,dt' \quad (10)$$

for $v = 2$,

$$(I_1 - I^0_1)/\int_0^t I_2\,dt' = k_{21}\frac{\alpha_1}{\alpha_2} - (k_{10} + k_d)(\int_0^t I_1\,dt'/\int_0^t I_2\,dt') \quad (11)$$

for $v = 1$, and

$$(I_0 - I^0_0)/\int_0^t I_2\,dt' = k_{20}\frac{\alpha_0}{\alpha_2} + k_{10}\frac{\alpha_0}{\alpha_1}(\int_0^t I_1\,dt'/\int_0^t I_2\,dt') - k_d(\int_0^t I_0\,dt'/\int_0^t I_2\,dt') \quad (12)$$

for $v = 0$. Equations 10 and 11 are in principle equivalent to single-exponential and double-exponential analysis, respectively. Equation 11 offers an advantage in the analysis of the profiles with $k_{21} \approx k_{10} + k_d$.[46,47,49] Integrated values of the signal intensities are calculated by the trapezoid formula. Unequivocal determination of all the rate coefficients, k_{21}, k_{20}, k_{10}, and k_d, and relative detectivities, α_1/α_2, α_0/α_2, and α_0/α_1, are made from the partial regression coefficients of these equations. It should be noted that one of the detectivities is arbitrary, for example, $\alpha_2 = 1$, because relative concentrations instead of absolute concentrations are necessary. Populations in the levels $v \geq 3$ are too small to obtain the rate coefficients for level-to-level relaxation from $v \geq 3$ to $v \leq 2$, and consequently, only overall relaxation rate coefficients of $v \geq 3$ have been determined.

Figure 3 shows SO_2 pressure dependencies of the first-order deactivation rates of SO($v = 1-5$). The plots are made after subtraction of the rates of diffusion loss from total removal rates. The slopes of the straight line fit from regression analysis correspond to the bimolecular rate coefficients for deactivation of SO($X^3\Sigma^-$, v) by collisions with SO_2: $(4.7 \pm 0.5) \times 10^{-12}$, $(6.7 \pm 0.4) \times 10^{-12}$, $(7.2 \pm 0.7) \times 10^{-12}$, $(6.1 \pm 1.0) \times 10^{-12}$, and $(8.6 \pm 0.7) \times 10^{-12}$ in units of cm^3 molecule^{-1} s^{-1} for $v = 1$, 2, 3, 4, and 5, respectively (the quoted errors are 2σ). The time profiles of $v = 0-2$ are governed by processes 1 and 5, and the slopes give overall vibrational relaxation rate coefficients. For $v = 2$, relaxation rate coefficients specific to the final levels, k_{21} and k_{20}, have also been determined to be $(2.5 \pm 0.9) \times 10^{-12}$ and $(4.2 \pm 0.9) \times 10^{-12}$ cm^3 molecule^{-1} s^{-1}, respectively. Rate coefficients obtained in the present study are listed in Table 2.

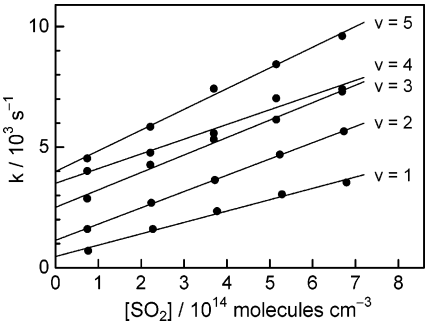

Figure 3. SO_2 pressure dependence of the first-order deactivation rates of $SO(X^3\Sigma^-, v = 1-5)$. Their slopes correspond to the rate coefficients for deactivation of $SO(v)$ by SO_2. The intercepts represent the deactivation rates of $SO(v)$ by N_2 at 50 Torr.

TABLE 2: Rate Constants for Vibrational Relaxation of $SO(X^3\Sigma^-, v = 1-5)$ by Collisions with SO_2[a]

$v = 1$	k_{10}[b]	$(4.7 \pm 0.5) \times 10^{-12}$
$v = 2$	k_{20}[b]	$(4.2 \pm 0.9) \times 10^{-12}$
	k_{21}[b]	$(2.5 \pm 0.9) \times 10^{-12}$
$v = 3$	k_3[c]	$(7.2 \pm 0.7) \times 10^{-12}$
$v = 4$	k_4[c]	$(6.1 \pm 1.0) \times 10^{-12}$
$v = 5$	k_5[c]	$(8.6 \pm 0.7) \times 10^{-12}$

[a] In units of cm^3 molecule^{-1} s^{-1}; the quoted errors are 2σ. [b] k_{ij} represents the rate constant for relaxation from $v = i$ to $v = j$. [c] Rate constants for overall deactivation.

Relative intensities of recorded time profiles $I_v/I_{v'}$ at time t are converted into relative concentrations $[v]/[v']$ using relative detectivities: $[v]/[v'] = (I_v/I_{v'})(\alpha_{v'}/\alpha_v)$; the observed profiles can, therefore, be so scaled as to make their ordinates common. The time evolutions of relative populations in $v = 0-2$ are shown in Figure 4 which is merely a small subset of the results. To ascertain that appropriate parameters are obtained in the analysis, fitting based on convolution was made. Rate equations for vibrational levels, which are inhomogeneous linear differential equations, can be solved by the well-known variation of parameters, and the following analytical solutions are obtained

$$[v] = [v]_0 \, e^{-k_v t} + \sum_{v'>v} (k_{v'v} \int_0^t [v'] \, e^{-k_v (t-x)} \, dx) \qquad (13)$$

where $v' = 1$ and 2 for $v = 0$ and $v' = 2$ for $v = 1$. The second term on the right side is called a convolution integral[45] which is also derived as an output from a linear system whose impulse response is $e^{-k_v t}$ [k_v is a first-order total removal rate (including diffusion loss) of a level v]. As shown in Figure 4, the observed time profiles are reproduced well at all pressures of SO_2.

There have been few quantitative studies on vibrational relaxation of $SO(X^3\Sigma^-)$. Kolbe and Leskovar[8] have detected vibrational levels of $SO(X^3\Sigma^-)$ by millimeter-wave spectroscopy, reporting that relaxation of $v = 2$ by SO_2 and Ar is faster than that of $v = 1$, which is qualitatively in agreement with our results. Gong et al.[50] have employed time-resolved FTIR emission spectroscopy to detect vibrationally excited $SO(X^3\Sigma^-)$ and determined rate coefficients of vibrational relaxation by SO_2 of $(1.5 \pm 0.3) \times 10^{-12}$ cm^3 molecule^{-1} s^{-1} on the assumption of single-quantum relaxation. Their value is smaller than those obtained in the present study by a factor of 3 ($v = 1$) to 6 ($v = 5$). They did not detect emission specific to a single vibrational level and gave averaged rate coefficients over the vibrational levels generated in the photolysis of SO_2 at 193 nm. Also, the IR emission from SO partly overlapped with that from $SO_2(\nu_1 = 1)$. It might be suggested that the spectroscopic interference is a cause of the discrepancy between the rate constants, although this is by no means certain.

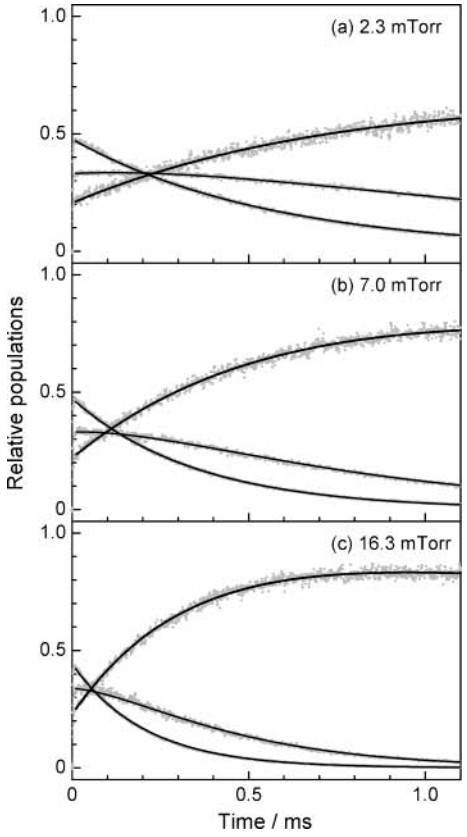

Figure 4. Time evolutions of concentration profiles of $SO(v = 0-2)$ at different SO_2 pressures. $P_{SO_2} = 2.3$ mTorr, (a); 7.0 mTorr, (b); 16.3 mTorr, (c). $P_{total}(N_2) = 50$ Torr. The ordinates are common to all the vibrational levels, and the profiles are so depicted as to make the sum of populations of $v = 0-2$ unity. The gray dots are observed signals, and the black lines represent fitting curves obtained by analytical solutions given by eq 13.

The order of the rate coefficients determined in the present study may reflect near-resonant $V-V$ energy transfer from $SO(v)$ to SO_2. The following propensities are derived by a simple theory of energy transfer:[51] (i) the selection rule for vibrational relaxation of a harmonic oscillator is $\Delta v = 1$; (ii) transition probabilities for energy transfer increase with vibrational quantum numbers; (iii) the efficiency of $V-V$ energy transfer is strongly dependent on the energy mismatch between the vibrational quantum energies; a small energy defect leads to fast energy transfer. The vibrational quantum energies of $SO(X^3\Sigma^-, v = 1-5)$ are 1138−1087 cm^{-1},[33] and these levels can be dealt with as a harmonic oscillator as a result of the small anharmonicity $\omega_e x_e = 6.3773$ cm^{-1}.[33] The vibrational quantum energies of SO_2 are 1151.4 (ν_1), 517.7 (ν_2), and 1361.8 cm^{-1} (ν_3);[52] the ν_1 vibration of SO_2 is, therefore, a likely mode for accepting the vibrational energy of $SO(v)$ as long as single-quantum relaxation ($\Delta v = 1$) occurs exclusively. However, the overall vibrational relaxation rate coefficients obtained in the present study show a smaller dependence on vibrational quantum number than expected. Furthermore, we have found that 63% of the deactivations of $v = 2$ proceed via double-quantum relaxation. The energy defect ΔE of double-quantum relaxation, $SO(v = 2) + SO_2 \rightarrow SO(v = 0) + SO_2(\nu_1 = 2) + \Delta E$, is 40 cm^{-1} which is larger than 13 cm^{-1} for single-quantum relaxation. The findings cannot be explained by the simple $V-V$ energy transfer between $SO(v)$ and SO_2. It should be noted that the propensities derived by the theory of energy transfer are based on an exponential repulsive interaction between colliding

TABLE 3: Nascent Vibrational Distributions of SO($X^3\Sigma^-$) Generated in the Photolysis of SO_2 at 193.3 nm[a]

$v=0$	$v=1$	$v=2$	$v=3$	$v=4$	$v=5$	condition	detection	refs
0.27	0.55	1.0	0.43	0.05		beam	TOF[b]	9
0.07	0.34	1.0	0.07			beam	TOF	10
0.07	0.30	1.0				beam	TOF	12
0[c]	0.3	1.0	< 0.07	0[c]	< 0.1	bulk	IR[d]	7
0.56	0.87	1.0	0.08	*e*	0.05	bulk	MW[f]	8
0.09	0.30	1.0	0	0	0	bulk	LIF[g]	11
0.52 ± 0.1	0.75 ± 0.1	1.0	*h*	*h*	*h*	bulk	LIF[i]	this work

[a] Normalized with population in $v=2$: $[v]_0/[v=2]_0$. [b] Time-of-flight mass. [c] No population was assumed. [d] Infrared absorption. [e] No measurement was made. [f] Millimeter-wave absorption. [g] Laser-induced fluorescence (LIF) via the $A^3\Pi-X^3\Sigma^-$ system. [h] Detected. [i] LIF via the $B^3\Sigma-X^3\Sigma^-$ system.

molecules,[51,53] and these are not always applicable to the cases where attractive interactions are important.

We have performed ab initio calculations[54] and found two triplet complexes S_2O_3: OS−OSO and SO−SO_2, both of which are $^3A''$ states. The energies of the complexes, calculated with UCCSD(Full,T)/aug-cc-pVTZ+1//B3LYP/aug-cc-pVTZ+1,[55] are lower than those of the reactants (SO + SO_2) by −8.7 kJ mol^{-1} (OS−OSO) and −12.3 kJ mol^{-1} (SO−SO_2) with zero-point energy correction. The nonexponential potentials with the attractive interactions increase the probability of the quantum number change with $\Delta v \geq 2$. It may, therefore, be suggested that vibrational relaxation of SO by SO_2 proceeds via transient complexes:

$$\mathrm{SO}(v) + \mathrm{SO_2} \rightarrow [\mathrm{S_2O_3}] \rightarrow \mathrm{SO}(v - \Delta v) + \mathrm{SO_2} \quad (\Delta v \geq 1) \quad (14)$$

The intercepts of Figure 3 correspond to the first-order deactivation rates of SO(v) by N_2 at 50 Torr. Quantitative results on deactivation by N_2 are not obtained, because the errors of the intercepts are large and because no measurements at different total pressures were made in the present study. Nevertheless, the rate coefficients of deactivation of SO(v) by N_2 monotonically increase with quantum number v, from 3×10^{-16} to 2.5×10^{-15} cm^3 molecule^{-1} s^{-1} for $v = 1-5$, suggesting that relaxation of SO(v) by N_2 is governed by a slow $V-T$ mechanism.

Nascent Vibrational Populations of SO Generated in the Photolysis of SO_2 at 193.3 nm. Relative detectivities, that is, nascent populations, were dealt with as variables instead of constants in the analysis; nevertheless, all the relative populations present at the time immediately after the photolysis were little dependent on SO_2 pressures (Figure 4). The initial relative populations in $v = 0-2$ determined at different SO_2 pressures have been averaged, and the resultant distributions are 0.52 ± 0.1/0.75 ± 0.1/1.0 for $v = 0/1/2$. Nascent populations in $v = 3-5$, on the other hand, cannot be determined, because neither relative detectivities among $v = 3-5$ nor the rate coefficients for relaxation from $v \geq 3$ to $v \leq 2$ are obtained. The nascent vibrational populations are listed in Table 3 together with the previously reported values. There are large discrepancies in vibrational distributions measured in bulk experiments. Kanamori et al.[7] employed infrared absorption spectroscopy and measured the differences instead of the ratios of populations in adjacent vibrational levels. They assumed no population in $v = 0$, which led to the underestimation of the population in $v = 1$. Chen et al.[11] detected SO by the LIF technique, and their spectra (Figure 1 in ref 11) show peaks assignable to the $v'-3$ and $v'-4$ bands in the $B^3\Sigma^- - X^3\Sigma^-$ system, indicating generation of $v = 3$ and 4; nevertheless, they assigned the spectra to rovibrational transitions only via the $A^3\Pi-X^3\Sigma^-$ system. Their conclusion that there were no populations in $v \geq 3$ and small populations in $v = 0$ and 1 might be due partly to the incorrect assignment of the spectra. Relative populations given by Kolbe and Leskovar[8] are in good agreement with ours despite different detection technique. Although no measurement was made for $v = 4$ in their study, evidence of the generation of $v = 4$ is given by the present study. Unfortunately, we were not able to determine the relative populations in $v \geq 3$ because of little correlation of the profiles among the levels $v \leq 2$ and $v \geq 3$. The fact indicates sufficiently small populations in $v \geq 3$ compared to those in $v \leq 2$, which is consistent with the results reported by the previous studies.

Kawasaki et al.[6,9] and Felder et al.[10,12] have employed the photofragment TOF mass spectroscopy. Both groups have reported that $v = 2$ has the largest population, although distributions derived by Kawasaki et al. are broader than those of Feler et al. The difference in distributions might reflect the difference in the temperature of parent SO_2. Kawasaki et al.[6] reported the temperature of rotation of SO_2 in a molecular beam to be 50−100 K and that of vibration to be 100−200 K. Felder et al.,[12] on the other hand, measured translational temperature to be 2 K instead of the temperatures of rotation and vibration. In general, rotational temperature in a molecular beam is close to that of translation, and consequently, the rotational and vibrational temperatures of SO_2 in the experiments by Felder et al. might be much lower than those by Kawasaki et al. The relatively high temperature of parent SO_2 in the study of Kawasaki et al. can be a cause of the broad vibrational distributions similar to those measured by the bulk experiments at room temperature. The line widths of the light at 193 nm from excimer lasers used in all the studies are nearly identical, and thus the large difference under the two conditions is the temperature of the parent SO_2: 298 K in bulk experiments[7,8] and < 100 K in beam experiments.[6,9,10,12] The thermal population in the low-lying ν_2 mode (517.7 cm^{-1}) of SO_2 at 298 K is larger than that at 100 K by a factor of 140. Vibrational excitation prior to photoexcitation could influence the dissociation dynamics.[56,57]

Not only vibration but also rotation might be a cause of the difference in the vibrational distributions reported under beam and bulk conditions. Ebata et al.[58] recorded the fluorescence excitation spectra of SO_2 via the $\tilde{C}^1B_2-\tilde{X}^1A_1$ system. They compared spectra recorded under different conditions (at room temperature and in a supersonic free jet) and reported that the fluorescence quantum yield is smaller at higher rotational levels. Their observations suggest that higher rotational levels are likely to couple with dissociating potentials, and as a consequence, the photodissociation mechanism might be different at high and low rotational levels of parent SO_2.

Cosofret et al.[59] have recently studied the photolysis of SO_2 between 202 and 207 nm by a resonance-enhanced multiphoton ionization TOF product-imaging technique, reporting that the nascent vibrational distributions of SO are strongly dependent on the initially prepared excited state of SO_2. Photolysis at

wavelengths different by only about 1 nm ($\Delta\tilde{\nu} = 300$ cm^{-1}) provided a large change in the product vibrational distributions: most of the populations are in $v = 0$ for wavelengths shorter than 203 nm, and $v = 0-2$ are evenly populated in dissociation at wavelengths longer than 203 nm. The difference was attributed to avoided crossing with repulsive ^{1}A′ surface below 203 nm. It might be suggested that there are also different dissociation mechanisms at around 193 nm: product distributions under beam conditions reflect a single dissociation dynamics, and at least two different dissociation mechanisms are responsible for the photolysis under bulk conditions.

Summary

This paper describes the study of the vibrational relaxation of SO($X^3\Sigma^-$, $v = 1-5$) by collisions with SO_2. Kinetic analysis of the time profiles of the LIF intensities was made using the integrated-profiles method. We have found the following features: (i) the vibrational level dependence of the deactivation rate coefficients is small and (ii) 63% of the relaxations of $v = 2$ by SO_2 proceed via double-quantum relaxation ($v = 2 \rightarrow v = 0$). These findings are explained by the attractive interactions between SO and SO_2. We have actually found two stable complexes, OS−OSO and SO−SO_2, by ab initio calculations. The relative populations of $v = 0-2$ immediately following the photolysis have also been determined to be $0.52 \pm 0.1/0.75 \pm 0.1/1.0$ for $v = 0/1/2$. The distribution is broader than those reported by beam experiments (0.07/0.3/1.0 for $v = 0/1/2$). The difference in the distributions measured by the two techniques is attributed to the difference in the temperature of the parent SO_2.

Acknowledgment. The authors gratefully acknowledge Craig A. Taatjes (Sandia National Laboratory) for invaluable comments. This work was supported by the Grant-in-Aid for Scientific Research on Priority Areas "Free Radical Science" (Contract No. 05237106), Grant-in-Aid for Scientific Research (B) (Contract No. 08454181), Grant-in-Aid for Scientific Research (C) (Contract No. 10640486), and Grant-in-Aid for Exploratory Research (Contract No. 15655005) of the Ministry of Education, Science, Sports, and Culture, Japan. Support also was provided by the Uchida Energy Science Promotion Foundation (No. 220117).

References and Notes

(1) Luther, K.; Troe, J. *17th International Symposium on Combustion*; Combustion Institute: Pittsburgh, PA, 1979; p 535.
(2) Brasseur, G. P.; Solomon, S. *Aeronomy of the Middle Atmosphere*; Reidel: Dordrecht, 1986.
(3) Dalgarno, A. In *Rate Coefficients in Astrochemistry*; Millar, T. J., Williams, D. A., Eds; Kluwer: Dordrecht, 1988; pp 321−338.
(4) Neufeld, D. A.; Dalgarno, A. *Astrophys. J.* **1989**, *340*, 869.
(5) Freedman, A.; Yang, S.-C.; Bersohn, R. *J. Chem. Phys.* **1979**, *70*, 5313.
(6) Kawasaki, M.; Kasatani, K.; Sato, H.; Shinohara, H.; Nishi, N. *Chem. Phys.* **1982**, *73*, 377.
(7) Kanamori, H.; Butler, J. E.; Kawaguchi, K.; Yamada, C.; Hirota, E. *J. Chem. Phys.* **1985**, *83*, 611.
(8) Kolbe, W. F.; Leskovar, B. *J. Chem. Phys.* **1986**, *85*, 7117.
(9) Kawasaki, M.; Sato, H. *Chem. Phys. Lett.* **1987**, *139*, 585.
(10) Felder, P.; Effenhauser, C. S.; Haas, B.-M.; Huber, J. R. *Chem. Phys. Lett.* **1988**, *148*, 417.
(11) Chen, X.; Asmar, F.; Wang, H.; Weiner, B. R. *J. Phys. Chem.* **1991**, *95*, 6415.
(12) Felder, P.; Haas, B.-M.; Huber, J. R. *Chem. Phys. Lett.* **1993**, *204*, 248.
(13) Yamasaki, K.; Taketani, F.; Tomita, S.; Sugiura, K.; Tokue, I. *J. Phys. Chem. A* **2003**, *107*, 2442.
(14) Stuart, B. C.; Cameron, S. M.; Powell, H. T. *J. Phys. Chem.* **1994**, *98*, 11499.
(15) Smith, W. H. *Astrophys. J.* **1972**, *176*, 265.
(16) Clyne, M. A. A.; McDermid, I. S. *J. Chem. Soc., Faraday Trans. 2* **1979**, *75*, 905.
(17) Herzberg, G. *Molecular Spectra and Molecular Structure, IV. Constants of Diatomic Molecules*; Van Nostrand Reinhold: New York, 1979.
(18) Krause, H. F. *Chem. Phys. Lett.* **1981**, *83*, 165.
(19) Colin, R. *J. Chem. Soc., Faraday Trans. 2* **1982**, *78*, 1139.
(20) Clyne, M. A. A.; Liddy, J. P. *J. Chem. Soc., Faraday Trans. 2* **1982**, *78*, 1127.
(21) Wu, K. T.; Morgner, H.; Yencha, A. J. *Chem. Phys.* **1982**, *68*, 285.
(22) Dorthe, G.; Costes, M.; Burdenski, S.; Caille, J.; Caubet, Ph. *Chem. Phys. Lett.* **1983**, *94*, 404.
(23) Cao, D.-Z.; Setser, D. W. *Chem. Phys. Lett.* **1985**, *116*, 363.
(24) Clyne, M. A. A.; Tennyson, P. H. *J. Chem. Soc., Faraday Trans. 2* **1986**, *82*, 1315.
(25) Johnson, C. A. F.; Kelly, S. D.; Parker, J. E. *J. Chem. Soc., Faraday Trans. 2* **1987**, *83*, 985.
(26) Cao, D.-Z.; Setser, D. W. *J. Phys. Chem.* **1988**, *92*, 1169.
(27) Lo, G.; Beaman, R.; Setser, D. W. *Chem. Phys. Lett.* **1988**, *149*, 384.
(28) Kulander, K. C. *Chem. Phys. Lett.* **1988**, *149*, 392.
(29) McAuliffe, M. J.; Bohn, M.; Dorko, E. A. *Chem. Phys. Lett.* **1990**, *167*, 27.
(30) Stuart, B. C.; Cameron, S. M.; Powell, H. T. *Chem. Phys. Lett.* **1992**, *191*, 273.
(31) Okabe, H. *Photochemistry of Small Molecules*; Wiley: New York, 1978.
(32) Calvert, J. G.; Pitts, J. N., Jr. *Photochemistry*; John Wiley and Sons: New York, 1966.
(33) Clerbaux, C.; Colin, R. *J. Mol. Spectrosc.* **1994**, *165*, 334.
(34) Martin, E. V. *Phys. Rev.* **1932**, *41*, 167.
(35) Tatum, J. B.; Watson, J. K. G. *Can. J. Phys.* **1971**, *49*, 2693.
(36) Herzberg, G. *Molecular Spectra and Molecular Structure, I. Spectra of Diatomic Molecules*; Van Nostrand Reinhold: New York, 1950.
(37) Katagiri, H.; Sako, T.; Hishikawa, A.; Yazaki, T.; Onda, K.; Yamanouchi, K.; Yoshino, K. *J. Mol. Struct.* **1997**, *413−414*, 589.
(38) Huang, Y.-L.; Gordon, R. J. *J. Chem. Phys.* **1990**, *93*, 868.
(39) Martinez, R. I.; Herron, J. T. *Int. J. Chem. Kinet.* **1983**, *15*, 1127.
(40) Herron, J. T.; Huie, R. E. *Chem. Phys. Lett.* **1980**, *76*, 322.
(41) Cobos, C. J.; Hippler, H.; Troe, J. *J. Phys. Chem.* **1985**, *89*, 1778.
(42) Borrell, P.; Cobos, C. J.; C. de Cobos, A. E.; Hippler, H.; Luther, K.; Ravishankara, A. R.; Troe, J. *Ber. Bunsen-Ges. Phys. Chem.* **1985**, *89*, 337.
(43) Singleton, D. L.; Cvetanovic, R. J. *J. Phys. Chem. Ref. Data* **1988**, *17*, 1377.
(44) Yamasaki, K.; Watanabe, A.; Kakuda, T.; Ichikawa, N.; Tokue, I. *J. Phys. Chem. A* **1999**, *103*, 451.
(45) Demas, J. N. *Excited State Lifetime Measurements*; Academic Press: New York, 1983.
(46) Yamasaki, K.; Watanabe, A. *Bull. Chem. Soc. Jpn.* **1997**, *70*, 89.
(47) Yamasaki, K.; Watanabe, A.; Kakuda, T.; Tokue, I. *Int. J. Chem. Kinet.* **1998**, *30*, 47.
(48) Yamasaki, K.; Watanabe, A.; Kakuda, T.; Tokue, I. *J. Phys. Chem. A* **2000**, *104*, 9081.
(49) Carrington, T. *Int. J. Chem. Kinet.* **1982**, *14*, 517.
(50) Gong, Y.; Makarov, V. I.; Weiner, B. R. *Chem. Phys. Lett.* **2003**, *378*, 493.
(51) Yardley, J. T. *Intramolecular Energy Transfer*; Academic Press: New York, 1980.
(52) Shimanouchi, T. *Tables of Molecular Vibrational Frequencies Consolidated Volume I*; National Bureau of Standards: Gaithersburg, MD, 1972; pp 1−160.
(53) The interaction potential is assumed to be an exponential repulsion of the form of $A \exp(-r/L)$, where A is a strength parameter, r is an intermolecular distance, and L is a range parameter (ref 51).
(54) Frisch, M. J.; Trucks, G. W.; Schlegel, H. B.; Scuseria, G. E.; Robb, M. A.; Cheeseman, J. R.; Zakrzewski, V. G.; Montgomery, J. A., Jr.; Stratmann, R. E.; Burant, J. C.; Dapprich, S.; Millam, J. M.; Daniels, A. D.; Kudin, K. N.; Strain, M. C.; Farkas, O.; Tomasi, J.; Barone, V.; Cossi, M.; Cammi, R.; Mennucci, B.; Pomelli, C.; Adamo, C.; Clifford, S.; Ochterski, J.; Petersson, G. A.; Ayala, P. Y.; Cui, Q.; Morokuma, K.; Malick, D. K.; Rabuck, A. D.; Raghavachari, K.; Foresman, J. B.; Cioslowski, J.; Ortiz, J. V.; Stefanov, B. B.; Liu, G.; Liashenko, A.; Piskorz, P.; Komaromi, I.; Gomperts, R.; Martin, R. L.; Fox, D. J.; Keith, T.; Al-Laham, M. A.; Peng, C. Y.; Nanayakkara, A.; Gonzalez, C.; Challacombe, M.; Gill, P. M. W.; Johnson, B. G.; Chen, W.; Wong, M. W.; Andres, J. L.; Head-Gordon, M.; Replogle, E. S.; Pople, J. A. *Gaussian 98*, revision A.9; Gaussian, Inc.: Pittsburgh, PA, 1998.
(55) The geometries of the complexes were optimized using the B3LYP hybrid density functional method and aug-cc-pVTZ+1 basis set. Unrestricted coupled-cluster single and double methods including the addition of perturbative contribution from connected triple excitations [CCSD(T)] were applied at the optimized geometries for determining accurate energies.
(56) Crim, F. F. *Annu. Rev. Phys. Chem.* **1993**, *44*, 397.
(57) Andreas, B.; Hutchison, J. M.; Holiday, R. J.; Crim, F. F. *J. Chem. Phys.* **2003**, *118*, 7144.
(58) Ebata, T.; Nakazawa, O.; Ito, M. *Chem. Phys. Lett.* **1988**, *143*, 31.
(59) Cosofret, B. R.; Dylewski, S. M.; Houston, P. L. *J. Phys. Chem. A* **2000**, *104*, 10240.